

# Comparison studies between BHBT<sub>2</sub>:PC<sub>71</sub>BM composite nanotubes and its bulk-heterojunction properties

Muhamad Doris<sup>1</sup>, Azzuliani Supangat<sup>1\*</sup>, Teh Chin Hoong<sup>1</sup>, Khaulah Sulaiman<sup>1</sup> and Rusli Daik<sup>2</sup>

## Abstract

In this study, we investigate the morphological, structural, and optical properties of both bulk-heterojunction and composite nanotubes that composed of thiophene-based small molecules 1,4-bis (2,2'-bithiopen-5-yl)2,5-dihexyloxybenzene (BHBT<sub>2</sub>) and fullerene [6,6]-phenyl C<sub>71</sub> butyric acid methyl ester (PC<sub>71</sub>BM). Mix-blended and template-assisted methods were used to fabricate the bulk-heterojunction and composite nanotubes, respectively. A single material of BHBT<sub>2</sub> thin films and nanotubes that fabricated via spin-coating and template-assisted methods, respectively, was also studied. Two different formations between bulk-heterojunction and composite nanotubes were compared to elaborate their advancement in properties. Absorption spectra of BHBT<sub>2</sub>:PC<sub>71</sub>BM bulk-heterojunction and composite nanotubes have fallen within the ultraviolet-visible (UV-vis) range. Field emission scanning electron microscope (FESEM) and high-resolution transmission electron microscope (HRTEM) images show that the carbon-rich of PC<sub>71</sub>BM, has successfully infiltrated into the BHBT<sub>2</sub> nanotube to form the BHBT<sub>2</sub>:PC<sub>71</sub>BM composite nanotubes. However, due to the informality distribution of infiltration, charge carrier transfer is seen to be better in bulk-heterojunction rather than in the composite nanotubes.

**Keywords:** Thiophene, alumina template, bulk-heterojunction, composite nanotube

---

\* Corresponding author: azzuliani@um.edu.my

<sup>1</sup> Low Dimensional Materials Research Centre, Department of Physics  
University of Malaya, Kuala Lumpur 50603, Malaysia

<sup>2</sup> School of Chemical Sciences and Food Technology, Faculty of Science and Technology, Universiti  
Kebangsaan Malaysia, 43600 UKM Bangi, Selangor, Malaysia

## Background

Organic materials have been the main interest to many of researchers due to their remarkable properties such as flexibility, abundance of resources, and low production cost. Initially, the organic materials are only used as the electric insulator of electronic devices. However, this practice has changed after the discovery of metallic behavior of polyacetylene (PA) by Shirakawa et.al [1]. The finding has uncovered the emergence of others conducting organic materials such as polythiophene (Pth), polypyrrole (PPY), polyaniline (PANI), polycarbazole (PCz), poly(3,4-ethylene dioxythiophene) (PEDOT), and polyfuran (PF) [2-9] that to date have been applied to numerous electronic devices. In addition, many others new organic materials are recently found and applied in electronic nanodevices (field effect transistor, light emitting diode) [10, 11], sensors (chemical, gas, optical, biosensor) [12-15], energy storage (solar cells, fuel cells, supercapacitors) [16-18], microwave absorption and electromagnetic shielding [19], and biomedical applications (drug delivery, protein purification, tissue engineering, neural interfaces, actuators) [20-24].

However, the small molecules based materials have the promising properties in terms of the viscoelasticity, toughness, crystallinity, and optical if compared to the polymer based materials [25-30]. Thiophene is a heterocyclic compound that consists of five-membered ring whose properties are still reliable and remarkable to date. Thiophene-based small molecules have shown extraordinary properties that may compete with its polymer in terms of enhancing efficiency to the perovskite-based solar cells and small molecules organic solar cells [28, 31]. Some applications such as small molecules organic solar cells [28, 30-32], inorganic-organic hybrid solar cells [33], and field effect transistor [34-36] have been realized from the thiophene-based small molecules. Therefore, the intensive studies of thiophene-based small molecules are as crucial as its thiophene-conjugated polymer. Thiophene-based small molecules, namely 1,4-bis (2,2'-bithiopen-5-yl)2,5-

dihexyloxybenzene (BHBT<sub>2</sub>) is a pentamer that consists of four thiophene rings and one benzene ring in which the benzene ring binds two hexyl molecules and the thiophene. BHBT<sub>2</sub> has a profound solubility particularly in organic solvents such as chloroform, dichloromethane, and tetrahydrofuran. In addition, it is easily purified through a column chromatography and recrystallization techniques. The terminal bithiophene groups in BHBT<sub>2</sub> pentamer is expected to provide a good stability and excellent charge transport properties in the pentamer backbone. Therefore, coupling of dihexyloxy-p-phenylene moiety with terminal bithiophene groups could improve the pi-electron conjugation path in the pentamer backbone without affecting the optical and electrochemical properties.

One of the crucial explorations of BHBT<sub>2</sub> properties is its nanostructures. Nanostructures of small molecules such as nanotubes, nanorods, nanowires, and nanoflowers have been commonly fabricated using template assisted-method [37-41]. The template is based on alumina oxide material that consists of orderly nanopores to infiltrate a solution, which in turn molds the nanostructured materials. Formation of nanostructures is important to be studied due to its exceptional properties over the planar structures. For instance, an active material in organic solar cells that fabricated into nanostructures with size corresponds to visible wavelength can enhance optical performance of the material [42]. In addition, nanostructuring an active material of solar cells into nanorods, nanotubes, and nanowires increases the surface area of active layer in absorbing more photons that results in higher efficiency [43, 44]. The template assisted-method is a low cost technique to produce nanostructured materials that the properties of the materials can easily be controlled [37, 45, 46]. The types of nanostructures are affected by the parameters of solution that infiltrate into the template's pores. Molecular weight, solution viscosity, solution concentration, infiltration mechanism, and drying process are some of the parameters that influence the formation of nanostructures [39, 40]. Template-assisted method can be used to fabricate the donor-

acceptor system of p-n junction composite nanotubes [47]. Unlike the well-known donor-acceptor system of bulk-heterojunction, the composite nanotubes that compose of ordered array of p-n core-shell junction could accommodate to the higher carriers mobility. p-n core-shell junction is widely used in applications such as in drug delivery and optoelectronic [48, 49]. Reported previously, a p-n core-shell junction nanowire that was applied to inorganic solar cells have improved the performance of device efficiency [44]. On top of that, p-n core-shell junction of composite nanotubes could also be able to enhance the charge carrier transfer if compared with its bulk-heterojunction [47].

In this study, the p-n core-shell junction of composite nanotubes has been successfully produced via template assisted-method. Composite nanotubes of BHBT<sub>2</sub> and fullerene [6,6]-phenyl C<sub>71</sub> butyric acid methyl ester (PC<sub>71</sub>BM) are fabricated and characterized. Characterizations are particularly emphasized on the optical, morphological, and structural properties of BHBT<sub>2</sub>:PC<sub>71</sub>BM. Two different formations of bulk-heterojunction and composite nanotubes of BHBT<sub>2</sub>:PC<sub>71</sub>BM are studied. To the best of our knowledge, there have been no studies that investigate the properties of thiophene-based small molecules BHBT<sub>2</sub>. Therefore, the studies on the p-n BHBT<sub>2</sub>:PC<sub>71</sub>BM properties may provide the informative and useful knowledge.

## Methods

Thiophene-based small molecules, 1,4-bis (2,2'-bithiophene-5-yl)2,5-dihexyloxybenzene (BHBT<sub>2</sub>) was synthesized and used directly as desired. As shown in Figure 1a, BHBT<sub>2</sub> contains of single benzene with four thiophene ring flank the benzene ring on each side. 5 mg of BHBT<sub>2</sub> was dissolved into the 1 ml of chloroform in which the solubility limit of BHBT<sub>2</sub> within chloroform is 59 mg ml<sup>-1</sup> [50]. Similar concentration of 5 mg/ml was applied for [6,6]-phenyl C<sub>71</sub> butyric acid methyl ester (PC<sub>71</sub>BM), by dissolving in chloroform. Volume ratio of 1:1 was used to produce the BHBT<sub>2</sub>:PC<sub>71</sub>BM bulk-heterojunction and composite nanotubes. Porous alumina template with 200 nm and 60 μm of pores diameter and thickness, respectively, was purchased from Whatman Anodisc and was utilized to fabricate nanostructures. Prior to the infiltration, templates were cleaned up by means of immerse it into acetone under sonication for 15 min, and then rinsed using deionized water. Three different spin coating rates of 1000, 2000, and 3000 rpm were used in 30 s. Prior to the spin coating process, template was firstly attached onto the glass slide by using scotch tape to its right and left side (Figure 1b). The scotch tape was used to hold the template to be stuck on the glass slide during the spin coating process. Figure 1c shows the infiltrated BHBT<sub>2</sub> after and before the spin coating and dissolution process, respectively.

Figure 2 represents the schematic illustrations on the formation of BHBT<sub>2</sub> nanotubes and BHBT<sub>2</sub>:PC<sub>71</sub>BM composite nanotubes. Porous alumina template was firstly cleaned up under sonication of acetone (i). Prior to the spin coating process, 50 μL of BHBT<sub>2</sub> solution was dropped onto the cleaned template, which then allow the solution to infiltrate into the template (ii). To fabricate the BHBT<sub>2</sub>:PC<sub>71</sub>BM composite nanotubes, 50 μL of PC<sub>71</sub>BM were dropped on top of the infiltrated BHBT<sub>2</sub> followed by the spin coating process (iii). Templates with infiltrated materials were then dried under the room temperature. These templates were stuck upside down on a copper tape (iv) before the dissolution of 6 h in 5 M of sodium

hydroxide (NaOH) was taken place (v). In order to fully wash out the remaining template, deionized water was used for rinse for several times. Finally, the obtained nanotubes that remain stuck on the copper tape are ready to be characterized (vi). Schematic illustrations shown in Figure 2 were adapted from the sample preparation set up shown in Figure 3. It is clearly seen that the infiltrated BHBT<sub>2</sub> shown a yellow appearance (Figure 3a). BHBT<sub>2</sub> nanotubes were able to retain their adhesion on the copper tape although the sample was washed for several times (Figure 3b). The colour of BHBT<sub>2</sub>:PC<sub>71</sub>BM composite nanotubes turned brownish due to the infiltration of PC<sub>71</sub>BM (Figure 3c). As portrayed by BHBT<sub>2</sub> nanotubes, BHBT<sub>2</sub>:PC<sub>71</sub>BM composite nanotubes were also able to stick upside down on copper tape after several washing (Figure 3d).

Several equipment such as spin coater model WS-650MZ-23NPP (Laurell Technologies Corp., North Wales, PA, USA), Field Emission Scanning Electron Microscope (FESEM) (Quanta FEG 450), High Resolution Transmission Electron Microscope (HRTEM) (Tecnai G2 FEI), Raman and photoluminescence spectroscopy (RENISHAW), UV-vis spectroscopy (Shimadzu UV-3101PC) and X-ray Diffraction Spectroscopy (XRD) were used in this studies.

## Results and discussion

In this study, investigation on the properties of single material and composite materials that consist BHBT<sub>2</sub> (p-type) and fullerene (n-type) are reported. BHBT<sub>2</sub> (1,4-bis (2,2'-bithiophene-5-yl)2,5-dihexyloxybenzene) is a novel small molecules with pentamer [50] with the advantage of high soluble with most solvents. By investigating its optical, morphological and structural properties, new applications within the organic electronics devices can be realized to improve the device performance. Based on the X-ray Diffraction (XRD) measurement of BHBT<sub>2</sub> shown in Figure 4a, multiple peaks that represent the BHBT<sub>2</sub> pristine indicate that the BHBT<sub>2</sub> small molecule is a crystalline material [51]. Crystalline material with periodic structure may provide a light management that can outperform devices, for instance, enhancement of photon absorption [52-54]. To elaborate the properties of BHBT<sub>2</sub> small molecules furthermore, incorporation between BHBT<sub>2</sub> and p-type material of PC<sub>71</sub>BM is applied. Nanostructuring these materials into p-n composite may enrich knowledge in nano-morphology studies. In addition, the charge transfer between donor and acceptor materials can be more understand and digest in providing information on the carriers behaviors. Figure 4b shows the energy diagram of BHBT<sub>2</sub> and PC<sub>71</sub>BM with HOMO-LUMO of 1.96-4.65 eV and 3.94-5.93 eV, respectively. HOMO-LUMO of donor-acceptor will enable the exciton (electron-hole) to dissociate at the interface [55].

### Optical properties studies

Figure 5a and Figure 5b show the absorption range of BHBT<sub>2</sub> thin films and nanotubes spin-coated at the different rates of 1000, 2000, and 3000 rpm, respectively. Similar pattern of absorption is shown with the dissimilarity in absorption intensity is only different. This can be understood that cause of the spin coating rate is matter to the thickness of material in which the thicker layer will attenuate the penetrated photon. From the UV-vis absorption

spectra, BHBT<sub>2</sub> thin films and nanotubes have portrayed five significant absorption peaks. There is no single peak shifted has taken place, due to the different spin coating rates, apart from the changes of absorption intensity of BHBT<sub>2</sub> nanotubes that get higher at 350 nm if compared to its thin films. It is noticed that BHBT<sub>2</sub> is favorably absorb photon only in the range of UV and visible light region. Due to its light absorption properties, BHBT<sub>2</sub> may potentially be applied as UV-vis photodetector or a booster material of active layer in organic photovoltaic applications. Fabricating this material into highly ordered nanostructures may enhance its performance since the charge carriers transfer mobility can be improved via the highly ordered structures [56, 57]. As shown in Figure 6a, BHBT<sub>2</sub> nanotubes reveal higher absorption intensity in comparison to their thin films [56]. BHBT<sub>2</sub> nanotubes and thin films exhibit four shoulders with their significant peaks occur at 335, 350, 414, 429, and 461 nm. The longer absorption wavelength of both BHBT<sub>2</sub> nanotubes and thin films are observed at 461 nm of Soret peak (B-band). This condition occur due to movement of an electron dipole that corresponds to nonbonding-antibonding (n-\*) excitation among BHBT<sub>2</sub> molecules. A small part of UV light that disclosed at around 320 - 350 nm is attributed to the bonding-antibonding ( $\pi$ -\*) excitation. Generally, nanostructuring the BHBT<sub>2</sub> either in single material or composite has increased its absorption performance. Incorporating BHBT<sub>2</sub> with PC<sub>71</sub>BM slightly shift the intense absorption and render the absorption range at 320-350 nm and 400-460 nm become broader. As shown in Figure 6b, although the presence of  $\pi$ -\* transition is observed in the BHBT<sub>2</sub> bulk-heterojunction, the better absorption is exhibited in the BHBT<sub>2</sub> composite nanotubes.

In an organic material, once a photon bombards onto a donor material, exciton which is a pair of electron-hole that bound with each other will be generated. In order to generate current, this exciton will need to be dissociated by dislodging the electron from its binding energy. One condition that has to be fulfilled is the affinity electron requirement of each



donor and acceptor materials. In our study, to investigate the potential application of BHBT<sub>2</sub> into device, BHBT<sub>2</sub> and electron acceptor of PC<sub>71</sub>BM is mixed. The HOMO-LUMO configuration of both materials should be possible to create a charge transfer phenomena since the electron affinity of acceptor material is bigger than the donor. Charge carriers transfer will only occur when the binding energy of exciton is lower than the electron affinity energy difference between donor and acceptor material [58].

Photoluminescence (PL) measurement is done to investigate the effectiveness of charge transfer between donor and acceptor. On the other words, photoluminescence provide information on how well can the exciton to reach donor-acceptor interfaces [59]. Exciton (pair of electron-hole) that has been generated by the donor material needs to be separated for the current extraction. Recombination of exciton will lead to the emission of radiative photon (radiative recombination) which is shown as intensity in the photoluminescence spectra [60]. Excitons that have successfully reached the donor-acceptor interfaces will be dissociated into hole and electron. This phenomenon can be indicated by the lower intensity exhibited by the photoluminescence peak (quenching) compared to the curve of radiative recombination which always exhibit the higher intensity. Quenching is attributed to the charge carriers transfer occurred between donor and acceptor that carriers are produced from the dissociated excitons at the donor-acceptor interfaces [59, 60]. As shown in Figure 7a, the quench phenomenon is occurred due to the incorporation between BHBT<sub>2</sub> and PC<sub>71</sub>BM, which allowed electrons from BHBT<sub>2</sub> to jump to the acceptor material. It is hardly to obtain the photoluminescence results for thin films that were spin-coated at 1000, 2000, and 3000 rpm with concentration of 5 mg/ml due to the thickness matter. To solve this hindrance, drop-casting of solution onto a glass substrate is applied in order to get the feasible films thickness. It is noticed that BHBT<sub>2</sub> thin films has a higher photoluminescence intensity compared to the BHBT<sub>2</sub> bulk-heterojunction and composite nanotubes. Mixing of two materials in the

formation of bulk-heterojunction and composite nanotubes has gained almost totally quenching. Figure 7b shows the photoluminescence spectra of BHBT<sub>2</sub> bulk-heterojunction and composite nanotubes. BHBT<sub>2</sub> bulk-heterojunction gets slightly quenched compared to its composite nanotubes. Charge transfer between BHBT<sub>2</sub> and PC<sub>71</sub>BM in the formation of bulk-heterojunction is more effective than the composite nanotubes. Base on the morphology view of bulk-heterojunction, donor and acceptor will easily agglomerate and mix together in order to allow the electron to reach the donor-acceptor interface. Better quenching of BHBT<sub>2</sub>:PC<sub>71</sub>BM bulk-heterojunction has a contradict result with what has been found by others [45, 47] where nanostructuring a material gets better quenching than bulk-heterojunction. Morphology of BHBT<sub>2</sub>:PC<sub>71</sub>BM composite nanotubes could be responsible for the better quenching of bulk-heterojunction where it could be predicted that most of interfaces of BHBT<sub>2</sub>:PC<sub>71</sub>BM composite nanotubes are unevenly constructed.

### **Structural properties studies**

Raman spectroscopy is applied to study the chemical and structural composition of materials. In its application, incident photons that interact with materials may lose or gain energy. The energy difference between the scattered photon and the incident photon is exactly similar to energy difference in molecular vibration. Therefore, the patterns of Raman spectra are generated from the molecular or lattice vibrations within the materials. A low frequency in Raman shift corresponds to a low energy vibration of atoms which means that heavy atoms are held together with the weak bonds. On the other hand, a high frequency is corresponded to light atoms which held together with strong bound [61]. Figure 8a and 8b show the Raman spectra of BHBT<sub>2</sub> thin films versus nanotubes and Raman spectra of BHBT<sub>2</sub>:PC<sub>71</sub>BM bulk-heterojunction versus composite nanotubes, respectively, with their Raman peaks are tabulated in Table 1. Raman peak at 1445 cm<sup>-1</sup> shows a slightly different in intensity between BHBT<sub>2</sub> thin films and nanotubes indicating that thiophenes ring are dominantly stretching in

thin film compared to its nanotubes. The occurrence of thiophenes ring stretching supports the existence of BHBT<sub>2</sub> molecular structure with four thiophene rings is attached to one benzene ring. However, the incorporation of two materials has resulted shifting around 3 cm<sup>-1</sup> to the lower frequency. This shifting could be due to the effect of incidence energy that is divided and served to the two different molecules, which in turn decreasing in scattered energy [61]. Most of the Raman peaks of BHBT<sub>2</sub> nanotubes are shifted to higher frequencies except for the peak at 1564 cm<sup>-1</sup> that has shifted to lower frequency for 2 cm<sup>-1</sup>. However, there is no CH deformation occurred in BHBT<sub>2</sub> nanotubes. Ring breathing and ring vibration para-substituted benzene are formed from the incorporation of BHBT<sub>2</sub> and PC<sub>71</sub>BM. These rings are found at 1188 cm<sup>-1</sup> and 1227 cm<sup>-1</sup>, respectively. BHBT<sub>2</sub> composite nanotubes have shown shifting to the higher frequencies of 1189 cm<sup>-1</sup>, and 1231 cm<sup>-1</sup>. Among the four Raman spectra (BHBT<sub>2</sub> thin films, BHBT nanotubes, BHBT<sub>2</sub>:PC<sub>71</sub>BM bulk heterojunction, and BHBT<sub>2</sub>:PC<sub>71</sub>BM composite nanotubes), BHBT nanotubes and BHBT<sub>2</sub>:PC<sub>71</sub>BM composite nanotubes have somewhat a similar intensity although the highest peak intensity is dominated by BHBT<sub>2</sub> thin films.

### **Formation of nanostructured composite**

BHBT<sub>2</sub> nanotubes have been synthesized via the template-assisted method. Figure 9a-c show the FESEM images of BHBT<sub>2</sub> nanotubes obtained from the three different spin coating rates of 1000, 2000, and 3000 rpm. Generally, the nanostructures create bundles of nanotubes by collapsing their tips with each other instead of grown aligned as a single nanotube. Formation of nanotubes bundles could be due to the presence of attractive forces (van der Waals interactions) between the nanotubes [40]. At spin coating rate of 1000 rpm, the morphology of BHBT<sub>2</sub> nanotubes are produced inconsistently with some of the tubes are longer than others. However, with the increase of spin coating rate to 2000 rpm, the homogeneous growth

of BHBT<sub>2</sub> nanotubes is attained. Further increase to 3000 rpm, has caused to the thicker base layer and denser nanotubes. Due to the thicker base layer, observation on the nanotubes bundles becomes very intricate as the base layer almost covered the nanotubes' structure. In the further investigation, spin coating rate at 2000 rpm is considered as an optimum parameter for the fabrication of BHBT<sub>2</sub>:PC<sub>71</sub>BM composites.

During the infiltration, solution that passes through the template nanochannels may experience two possible conditions along the process. The first possible condition is the solution will spread and wet over the nanochannels' wall which in turn produce the hollow nanotubes after the template dissolution. The other possible condition is the formation of nanorods, that due to the existence of force interaction between the molecules (solution) during infiltration which stronger than the adhesive force (wall). In this study, the growth mechanism of BHBT<sub>2</sub> nanostructures is portrayed by the first possible condition (Figure 10 a-d). Since the optimum spin coating rate is 2000 rpm (BHBT<sub>2</sub> nanotubes), BHBT<sub>2</sub>:PC<sub>71</sub>BM composite nanotubes are then produced at this optimum rate. Observation of hollow structure has supported the prediction of wall wetting and force interaction between the wall and solution. The wall of BHBT<sub>2</sub>:PC<sub>71</sub>BM composite nanotubes are thicker than the BHBT<sub>2</sub> nanotubes due to the infiltration of two different materials (BHBT<sub>2</sub> and PC<sub>71</sub>BM).

Figure 11a and 11b show the HRTEM images of BHBT<sub>2</sub> nanotubes and BHBT<sub>2</sub>:PC<sub>71</sub>BM composite nanotubes, respectively. BHBT<sub>2</sub> nanotubes contain only single wall of tube whereas BHBT<sub>2</sub>:PC<sub>71</sub>BM composite nanotubes exhibit two different regions. These two different regions are corresponded to the PC<sub>71</sub>BM (inner) and BHBT<sub>2</sub> (outer), respectively. PC<sub>71</sub>BM is infiltrated into the center of hollow BHBT<sub>2</sub> which is shown as a darker region. PC<sub>71</sub>BM of carbon rich materials has successfully infiltrated into the BHBT<sub>2</sub> nanotubes and wetted the inner wall of nanotubes which have led to the formation of p-n

junction. If assumption that all of the PC<sub>71</sub>BM has totally infiltrated into the BHBT<sub>2</sub> nanotubes is made, more effective charge transfer will be taken place in composite nanotubes rather than in the bulk-heterojunction. However, based on the morphological images, it is notice that not many PC<sub>71</sub>BM has been infiltrated into the BHBT<sub>2</sub> nanotubes. In addition to that, the size of nanotubes is not homogeneously constructed. The occurrence of this phenomenon may be due to the spin coating rate. In the spin coating process, some of the substances may have been swept away out of the alumina template surface. Ideally, PC<sub>71</sub>BM substances would have to fully infiltrate the BHBT<sub>2</sub> nanotubes in order to form the homogeneous composite nanotubes and to have a well-mixed of donor-acceptor interfaces. Therefore, the composite nanotubes would provide more effective way for the charges to be transferred into the acceptor material.

## **Conclusions**

We have successfully synthesized and characterized the properties of 1,4-bis (2,2'-bithiopen-5-yl)2,5-dihexyloxybenzene (BHBT<sub>2</sub>) as single material and composites. The comparison studies between BHBT<sub>2</sub> thin films, BHBT<sub>2</sub> nanotubes, BHBT<sub>2</sub>:PC<sub>71</sub>BM bulk-heterojunction and BHBT<sub>2</sub>:PC<sub>71</sub>BM composite nanotubes were emphasized on their optical, structural and morphological properties. Nanostructuring the BHBT<sub>2</sub> via template-assisted method has been successfully applied to produce nanotubes and composite nanotubes. Better quenching and improvement of charge carriers' transport is observed in BHBT<sub>2</sub>:PC<sub>71</sub>BM bulk-heterojunction due to the poor interfaces morphology of unevenly constructed BHBT<sub>2</sub>:PC<sub>71</sub>BM composite nanotubes. However, the enhancement of light absorption is observed in BHBT<sub>2</sub> nanotubes and BHBT<sub>2</sub>:PC<sub>71</sub>BM composite nanotubes. PC<sub>71</sub>BM has been successfully infiltrated into the BHBT<sub>2</sub> nanotubes due to the wetting properties possessed by both materials, although the uniformity of infiltration is poor.

## **Abbreviations**

BHBT<sub>2</sub>, 1,4-bis (2,2'-bithiopen-5-yl)2,5-dihexyloxybenzene; FESEM, field emission scanning electron microscopy; HOMO, highest occupied molecular orbital; HRTEM, high resolution transmission electron microscopy; LUMO, lowest unoccupied molecular orbital; NaOH, sodium hydroxide; PA, polyacetylene; PANI, polyaniline; PC<sub>71</sub>BM, [6,6]-phenyl C<sub>71</sub>-butyric acid methyl ester; PCz, polycarbazole; PEDOT, poly(3,4-ethylene dioxythiophene); PF, polyfuran; PL, photoluminescence; Pth, polythiophene; PPV, polyparaphenylene vinylene; PPY, polypyrrole; XRD, X-ray Diffraction Spectroscopy

## **Competing interests**

The authors declare that they have no competing interests.

## **Authors' contributions**

MD carried out the experiments, performed the analysis, and drafted the manuscript. AS participated in the design of the study, performed the analysis, and helped draft the manuscript. TCH carried out the experiments, and performed the analysis. KS and RD participated in the design of study and in the sequence alignment.

## **Authors' information**

MD is a research assistant and applying for postgraduate studies at the University of Malaya. TCH is currently a postdoctoral fellowship at the University of Malaya. AS and KS is the senior lecturer and associate professor at the Department of Physics, University of Malaya, respectively, while RD is a professor at the National University of Malaysia.

## Acknowledgements

The authors would like to acknowledge the University of Malaya for the project funding under the University of Malaya High Impact Research Grant UM-MoE (UM.S/625/3/HIR/MoE/SC/26), University Malaya Research Grant (RG283-14AFR), and the Ministry of Education Malaysia for the project funding under Fundamental Research Grant Scheme (FP002-2013A).

## References

1. Shirakawa H, Louis EJ, MacDiarmid AG, Chiang CK, Heeger AJ: **Synthesis of electrically conducting organic polymers: halogen derivatives of polyacetylene, (CH)**. *Journal of the Chemical Society, Chemical Communications* 1977, **16**:578-580.
2. Kirchmeyer S, Reuter K: **Scientific importance, properties and growing applications of poly(3,4-ethylenedioxythiophene)**. *Journal of Materials Chemistry* 2005, **15**(21):2077-2088.
3. Booth MA, Leveneur J, Costa AS, Kennedy J, Travas-Sejdic J: **Tailoring the Conductivity of Polypyrrole Films Using Low-Energy Platinum Ion Implantation**. *The Journal of Physical Chemistry C* 2012, **116**(14):8236-8242.
4. Ćirić-Marjanović G: **Recent advances in polyaniline research: Polymerization mechanisms, structural aspects, properties and applications**. *Synthetic Metals* 2013, **177**(0):1-47.
5. Chen Q, Liu DP, Zhu JH, Han BH: **Mesoporous Conjugated Polycarbazole with High Porosity via Structure Tuning**. *Macromolecules* 2014, **47**(17):5926-5931.
6. Bajpai M, Srivastava R, Dhar R, Tiwari RS, Chand S: **p-Type doping of tetrafluorotetracyanoquinodimethane (F4TCNQ) in poly(para-phenylene vinylene) (PPV) derivative "Super Yellow" (SY)**. *RSC Advances* 2014, **4**(88):47899-47905.
7. Sreeram A, Patel NG, Venkatanarayanan RI, McLaughlin JB, DeLuca SJ, Yuya PA, Krishnan S: **Nanomechanical properties of poly(para-phenylene vinylene) determined using quasi-static and dynamic nanoindentation**. *Polymer Testing* 2014, **37**(0):86-93.
8. Atanasov SE, Losego MD, Gong B, Sachet E, Maria J-P, Williams PS, Parsons GN: **Highly Conductive and Conformal Poly(3,4-ethylenedioxythiophene) (PEDOT) Thin Films via Oxidative Molecular Layer Deposition**. *Chemistry of Materials* 2014, **26**(11):3471-3478.
9. Sheberla D, Patra S, Wijsboom YH, Sharma S, Sheynin Y, Haj-Yahia A-E, Barak AH, Gidron O, Bendikov M: **Conducting polyfurans by electropolymerization of oligofurans**. *Chemical Science* 2015, **6**(1):360-371.
10. Lee SY, Choi GR, Lim H, Lee KM, Lee SK: **Electronic transport characteristics of electrolyte-gated conducting polyaniline nanowire field-effect transistors**. *Applied Physics Letters* 2009, **95**(1):013113.
11. Grimsdale AC, Leok Chan K, Martin RE, Jokisz PG, Holmes AB: **Synthesis of Light-Emitting Conjugated Polymers for Applications in Electroluminescent Devices**. *Chemical Reviews* 2009, **109**(3):897-1091.
12. Rajesh, Ahuja T, Kumar D: **Recent progress in the development of nano-structured conducting polymers/nanocomposites for sensor applications**. *Sensors and Actuators B: Chemical* 2009, **136**(1):275-286.

13. Menegazzo N, Herbert B, Banerji S, Booksh KS: **Discourse on the utilization of polyaniline coatings for surface plasmon resonance sensing of ammonia vapor.** *Talanta* 2011, **85**(3):1369-1375.
14. Michira I, Akinyeye R, Baker P, Iwuoha E: **Synthesis and Characterization of Sulfonated Polyanilines and Application in Construction of a Diazinon Biosensor.** *International Journal of Polymeric Materials and Polymeric Biomaterials* 2011, **60**(7):469-489.
15. Wang X, Shao M, Shao G, Fu Y, Wang S: **Reversible and efficient photocurrent switching of ultra-long polypyrrole nanowires.** *Synthetic Metals* 2009, **159**(3-4):273-276.
16. Fischer FSU, Trefz D, Back J, Kayunkid N, Tornow B, Albrecht S, Yager KG, Singh G, Karim A, Neher D, Brinkmann M, Ludwigs S: **Highly Crystalline Films of PCPDTBT with Branched Side Chains by Solvent Vapor Crystallization: Influence on Opto-Electronic Properties.** *Advanced Materials* 2015, **27**(7):1223-1228.
17. Ma Y, Jiang S, Jian G, Tao H, Yu L, Wang X, Wang X, Zhu J, Hu Z, Chen Y: **CNx nanofibers converted from polypyrrole nanowires as platinum support for methanol oxidation.** *Energy & Environmental Science* 2009, **2**(2):224-229.
18. Chen L, Yuan C, Dou H, Gao B, Chen S, Zhang X: **Synthesis and electrochemical capacitance of core-shell poly (3,4-ethylenedioxythiophene)/poly (sodium 4-styrenesulfonate)-modified multiwalled carbon nanotube nanocomposites.** *Electrochimica Acta* 2009, **54**(8):2335-2341.
19. Saini P, Choudhary V, Singh BP, Mathur RB, Dhawan SK: **Polyaniline-MWCNT nanocomposites for microwave absorption and EMI shielding.** *Materials Chemistry and Physics* 2009, **113**(2-3):919-926.
20. Kim S, Kim J-H, Jeon O, Kwon IC, Park K: **Engineered polymers for advanced drug delivery.** *European Journal of Pharmaceutics and Biopharmaceutics* 2009, **71**(3):420-430.
21. Zhu Y, Li J, Wan M, Jiang L: **Superhydrophobic 3D Microstructures Assembled From 1D Nanofibers of Polyaniline.** *Macromolecular Rapid Communications* 2008, **29**(3):239-243.
22. Srivastava S, Chakraborty A, Salunke R, Roy P: **Development of a Novel Polygalacturonic Acid-Gelatin Blend Scaffold Fabrication and Biocompatibility Studies for Tissue-Engineering Applications.** *International Journal of Polymeric Materials and Polymeric Biomaterials* 2012, **61**(9):679-698.
23. Kang G, Borgens RB, Cho Y: **Well-Ordered Porous Conductive Polypyrrole as a New Platform for Neural Interfaces.** *Langmuir* 2011, **27**(10):6179-6184.
24. Otero TF, Sanchez JJ, Martinez JG: **Biomimetic Dual Sensing-Actuators Based on Conducting Polymers. Galvanostatic Theoretical Model for Actuators Sensing Temperature.** *The Journal of Physical Chemistry B* 2012, **116**(17):5279-5290.
25. Fischer I, Kaeser A, Peters-Gumbs MAM, Schenning APHJ: **Fluorescent  $\pi$ -Conjugated Polymer Dots versus Self-Assembled Small-Molecule Nanoparticles: What's the Difference?.** *Chemistry – A European Journal* 2013, **19**(33):10928-10934.
26. Liu Y, Chen C-C, Hong Z, Gao J, Yang YM, Zhou H, Dou L, Li G, Yang Y: **Solution-processed small-molecule solar cells: breaking the 10% power conversion efficiency.** *Nature Scientific Reports* 2013, **3**:3356.
27. Zhang Q, Kan B, Liu F, Long G, Wan X, Chen X, Zuo Y, Ni W, Zhang H, Li M, Hu Z, Huang F, Cao Y, Liang Z, Zhang M, Russell TP, Chen Y: **Small-molecule solar cells with efficiency over 9%.** *Nat Photon* 2015, **9**(1):35-41.
28. Li H, Fu K, Boix PP, Wong LH, Hagfeldt A, Grätzel M, Mhaisalkar SG, Grimsdale AC: **Hole-Transporting Small Molecules Based on Thiophene Cores for High Efficiency Perovskite Solar Cells.** *ChemSusChem* 2014, **7**(12):3420-3425.
29. Mishra A, Bäuerle P: **Small Molecule Organic Semiconductors on the Move: Promises for Future Solar Energy Technology.** *Angewandte Chemie International Edition* 2012, **51**(9):2020-2067.



30. Zhou J, Wan X, Liu Y, Zuo Y, Li Z, He G, Long G, Ni W, Li C, Su X, Chen Y: **Small Molecules Based on Benzo[1,2-b:4,5-b']dithiophene Unit for High-Performance Solution-Processed Organic Solar Cells.** *Journal of the American Chemical Society* 2012, **134**(39):16345-16351.
31. Malytskyi V, Simon JJ, Patrone L, Raimundo JM: **Thiophene-based push-pull chromophores for small molecule organic solar cells (SMOSCs).** *RSC Advances* 2015, **5**(1):354-397.
32. Montcada NF, Pelado B, Viterisi A, Albero J, Coro J, Cruz Pdl, Langa F, Palomares E: **High open circuit voltage in efficient thiophene-based small molecule solution processed organic solar cells.** *Organic Electronics* 2013, **14**(11):2826-2832.
33. Freitas FS, Clifford JN, Palomares E, Nogueira AF: **Tailoring the interface using thiophene small molecules in TiO<sub>2</sub>/P3HT hybrid solar cells.** *Physical Chemistry Chemical Physics* 2012, **14**(34):11990-11993.
34. Park JI, Chung JW, Kim JY, Lee J, Jung JY, Koo B, Lee BL, Lee SW, Jin YW, Lee SY: **Dibenzothiopheno[6,5-b:6',5'-f]thieno[3,2-b]thiophene (DBTTT): High-Performance Small-Molecule Organic Semiconductor for Field-Effect Transistors.** *Journal of the American Chemical Society* 2015. doi:10.1021/jacs.5b01108
35. Sun J-P, Hendsbee AD, Eftaiha AaF, Macaulay C, Rutledge LR, Welch GC, Hill IG: **Phthalimide-thiophene-based conjugated organic small molecules with high electron mobility.** *Journal of Materials Chemistry C* 2014, **2**(14):2612-2621.
36. Wang C, Zang Y, Qin Y, Zhang Q, Sun Y, Di C-a, Xu W, Zhu D: **Thieno[3,2-b]thiophene-Diketopyrrolopyrrole-Based Quinoidal Small Molecules: Synthesis, Characterization, Redox Behavior, and n-Channel Organic Field-Effect Transistors.** *Chemistry – A European Journal* 2014, **20**(42):13755-13761.
37. Al-Kaysi RO, Ghaddar TH, Guirado G: **Fabrication of one-dimensional organic nanostructures using anodic aluminum oxide templates.** *Journal of Nanomaterials* 2009, Article ID 436375
38. Hu J, Shirai Y, Han L, Wakayama Y: **Template method for fabricating interdigitate p-n heterojunction for organic solar cell.** *Nanoscale Res Lett* 2012, **7**(1):1-5.
39. Fakir MS, Supangat A, Sulaiman K: **Templated growth of PFO-DBT nanorod bundles by spin coating: effect of spin coating rate on the morphological, structural, and optical properties.** *Nanoscale Res Lett* 2014, **9**(1):1-7.
40. Bakar NA, Supangat A, Sulaiman K: **Elaboration of PCDTBT nanorods and nanoflowers for augmented morphological and optical properties.** *Materials Letters* 2014, **131**:27-30.
41. Jung WS, Do YH, Kang MG, Kang CY: **Energy harvester using PZT nanotubes fabricated by template-assisted method.** *Current Applied Physics* 2013, **13**, Supplement 2 (0):S131-S134.
42. Edman Jonsson G, Fredriksson H, Sellappan R, Chakarov D: **Nanostructures for Enhanced Light Absorption in Solar Energy Devices.** *International Journal of Photoenergy* 2011, Article ID 939807.
43. Yu K, Chen J: **Enhancing solar cell efficiencies through 1-D nanostructures.** *Nanoscale Res Lett* 2009, **4**(1):1-10
44. Wang S, Yan X, Zhang X, Li J, Ren X: **Axially connected nanowire core-shell pn junctions: a composite structure for high-efficiency solar cells.** *Nanoscale Res Lett* 2015, **10**(1):1-7.
45. Supangat A, Kamarundzaman A, Bakar NA, Sulaiman K, Zulfiqar H: **P3HT: VOPcPhO composite nanorods arrays fabricated via template-assisted method: Enhancement on the structural and optical properties.** *Materials Letters* 2014, **118**:103-106.
46. Kamarundzaman A, Fakir MS, Supangat A, Sulaiman K, Zulfiqar H: **Morphological and optical properties of hierarchical tubular VOPcPhO nanoflowers.** *Materials Letters* 2013, **111**(0):13-16.
47. Makinudin AHA, Fakir MS, Supangat A: **Metal phthalocyanine: fullerene composite nanotubes via templating method for enhanced properties.** *Nanoscale Res Lett* 2015, **10**(1):1-8
48. Chatterjee K, Sarkar S, Jagajjanani Rao K, Paria S: **Core/shell nanoparticles in biomedical applications.** *Advances in Colloid and Interface Science* 2014, **209**(0):8-39.

49. Tchoulfian P, Donatini F, Levy F, Dussaigne A, Ferret P, Pernot J: **Direct Imaging of p–n Junction in Core–Shell GaN Wires.** *Nano letters* 2014, **14**(6):3491-3498
50. Wei LL, Hoong TC, Sulaiman K, Daik R, NM S: **Synthesis and Characterization of Solution Processable Organic Ultraviolet (UV) Photodetector based on 2,2'-Bithiophene End-Capped Dihexyloxy Phenylene Pentamer.** (will be published elsewhere)
51. Cullity BD: **Elements of X-ray diffraction.** 1978, Addison-Wesley, Philippines
52. Battaglia C, Hsu C-M, Söderström K, Escarré J, Haug F-J, Charrière M, Boccard M, Despeisse M, Alexander DTL, Cantoni M, Cui Y, Ballif C: **Light Trapping in Solar Cells: Can Periodic Beat Random?** *ACS Nano* 2012, **6**(3):2790-2797.
53. Sai H, Koida T, Matsui T, Yoshida I, Saito K, Kondo M: **Microcrystalline silicon solar cells with 10.5% efficiency realized by improved photon absorption via periodic textures and highly transparent conductive oxide.** *Applied Physics Express* 2013, **6**(10):104101.
54. Sai H, Kondo M, Saito K: **Periodic structures boost performance of thin-film solar cells.** <http://spie.org/x91297.xml>. Accessed 20 April 2015
55. Kietzke T: **Recent advances in organic solar cells.** *Advances in OptoElectronics* 2007, Article ID **40285**.
56. Kumar B, Kim SW: **Energy harvesting based on semiconducting piezoelectric ZnO nanostructures.** *Nano Energy* 2012, **1**(3):342-355.
57. Liang D, Kang Y, Huo Y, Chen Y, Cui Y, Harris JS: **High-efficiency nanostructured window GaAs solar cells.** *Nano letters* 2013, **13**(10):4850-4856
58. Abdulrazzaq OA, Saini V, Bourdo S, Dervishi E, Biris AS: **Organic solar cells: a review of materials, limitations, and possibilities for improvement.** *Particulate Science and Technology* 2013, **31**(5):427-442.
59. Cates NC, Gysel R, Beiley Z, Miller CE, Toney MF, Heeney M, McCulloch I, McGehee MD: **Tuning the properties of polymer bulk heterojunction solar cells by adjusting fullerene size to control intercalation.** *Nano letters* 2009, **9**(12):4153-4157.
60. Hoppe H, Niggemann M, Winder C, Kraut J, Hiesgen R, Hinsch A, Meissner D, Sariciftci NS: **Nanoscale morphology of conjugated polymer/fullerene-based bulk-heterojunction solar cells.** *Advanced Functional Materials* 2004, **14**(10):1005-1011.
61. Bright WE, Decius JC, Paul CC: **Molecular vibrations: the theory of infrared and raman vibrational spectra.** 1955, McGraw-Hill Book Company, Inc.
62. Francis RD, William GF, Freeman FB: **Characteristic Raman frequencies of organic compounds.** 1973, John Wiley & Sons Inc.

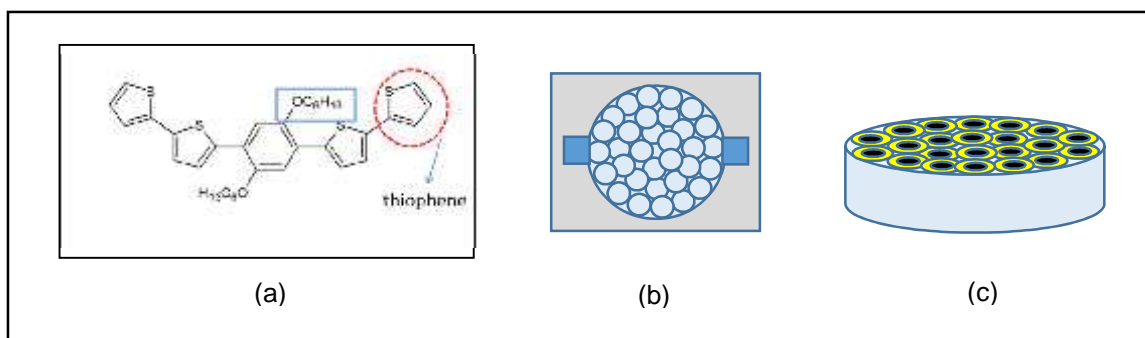


**Figure 1** (a) Molecular structure of BHBT<sub>2</sub>. (b) Illustration of porous alumina template being stuck on glass substrate. (c) Illustration of infiltrated BHBT<sub>2</sub>.

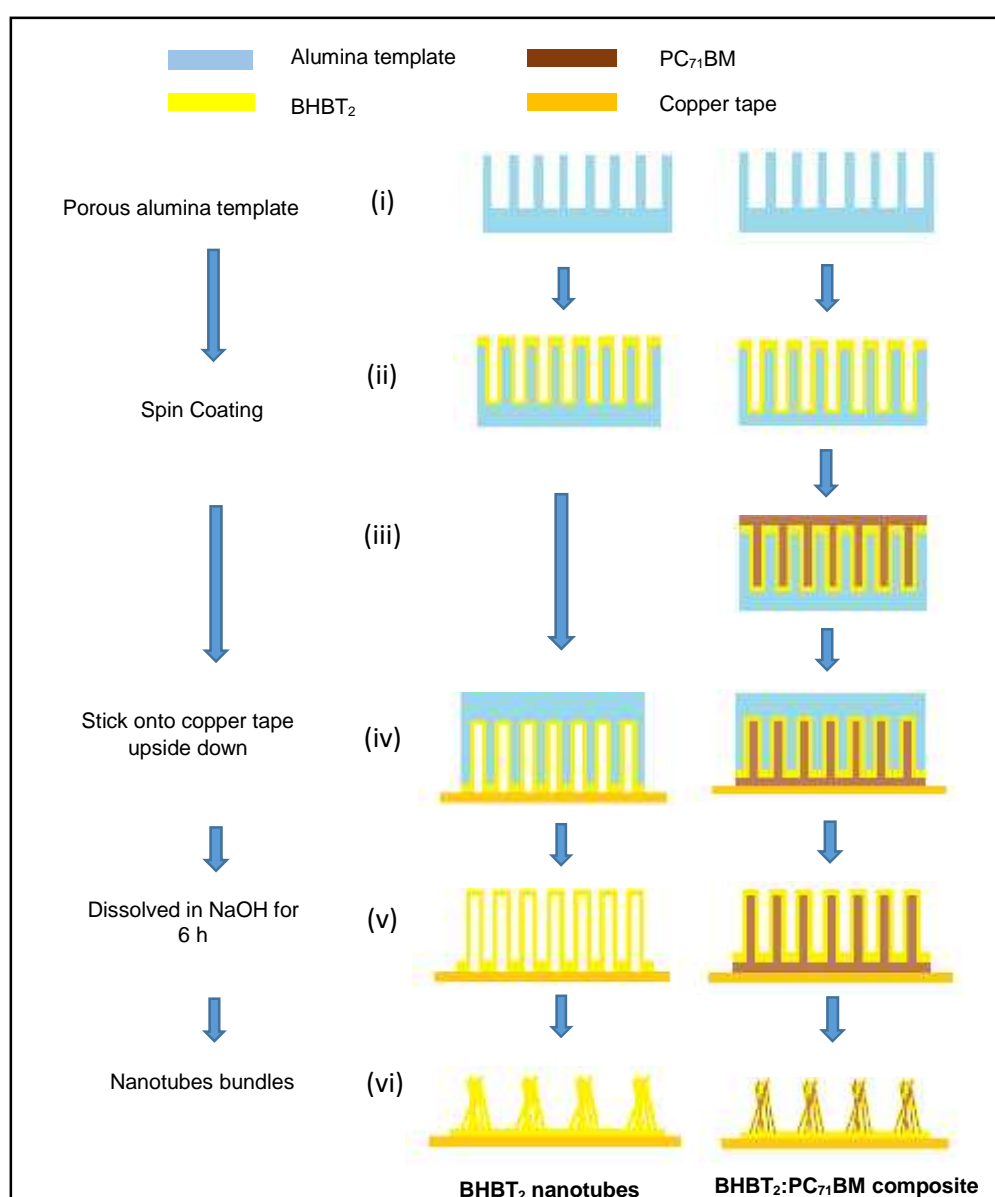


**Figure 2** Schematic illustrations on the formation of BHBT<sub>2</sub> nanotubes and BHBT<sub>2</sub>:PC<sub>71</sub>BM composite nanotubes.

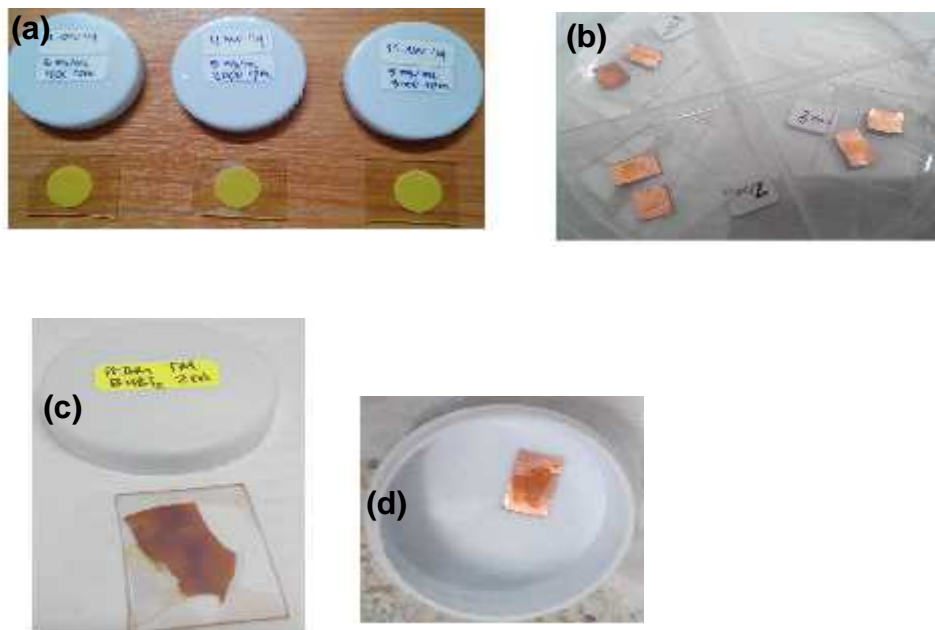


**Figure 3** (a) Infiltrated BHBT<sub>2</sub> that spin coated at three different rates of 1000, 2000 and 3000 rpm. (b) BHBT<sub>2</sub> nanotubes stick upside down on copper tape. (c) BHBT<sub>2</sub>:PC<sub>71</sub>BM composite nanotubes before dissolution. (d) BHBT<sub>2</sub>:PC<sub>71</sub>BM composite nanotubes stick upside down on copper tape.

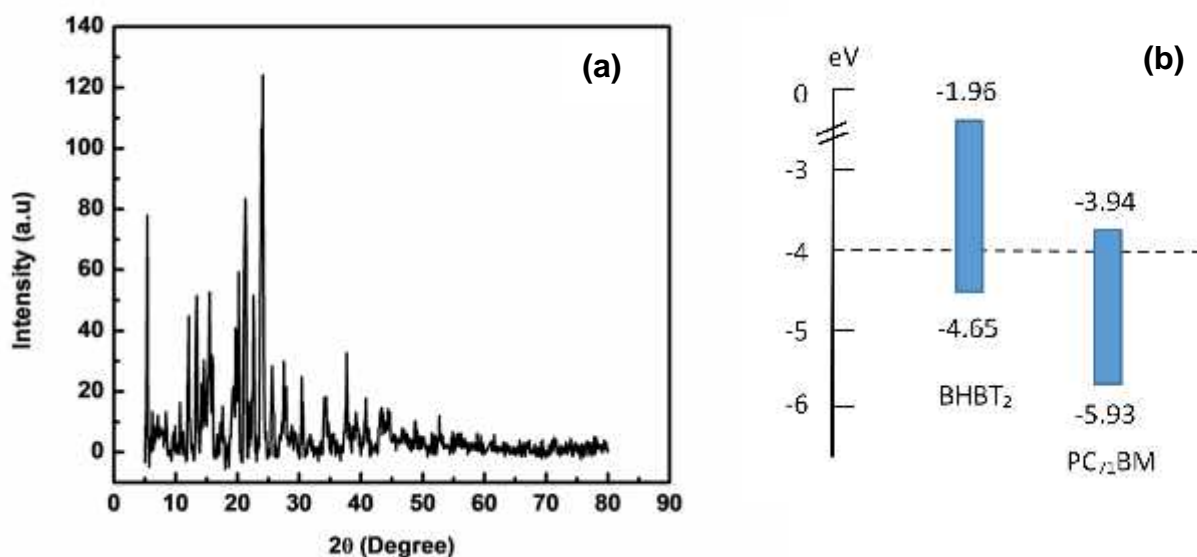


**Figure 4** (a) XRD measurement of pristine BHBT<sub>2</sub>. (b) Vacuum level (energy diagram) of BHBT<sub>2</sub> and PC<sub>71</sub>BM.

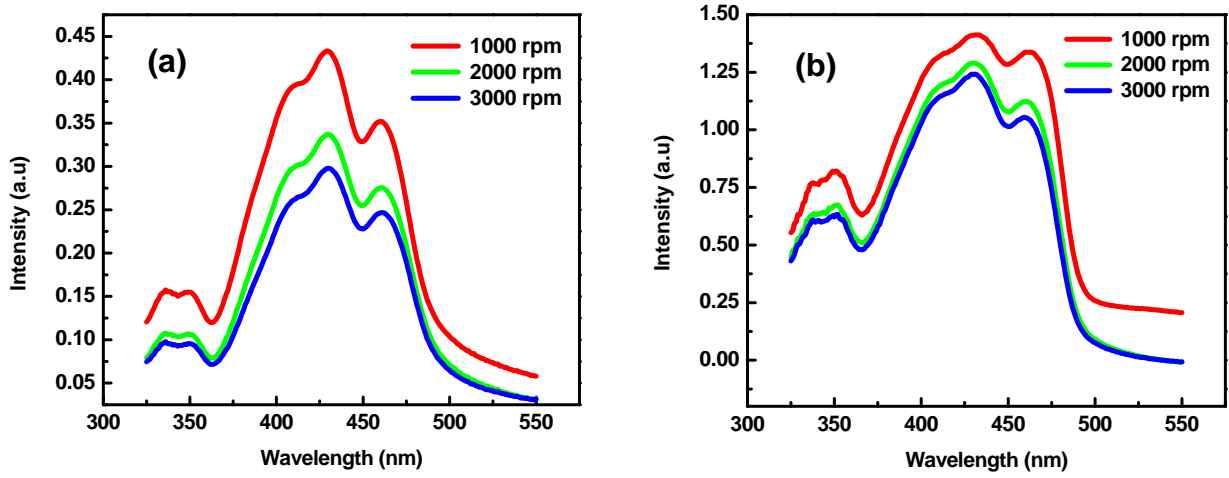


**Figure 5** (a) UV-vis absorption spectra of BHBT<sub>2</sub> thin films. (b) UV-vis absorption spectra of BHBT<sub>2</sub> nanotubes.

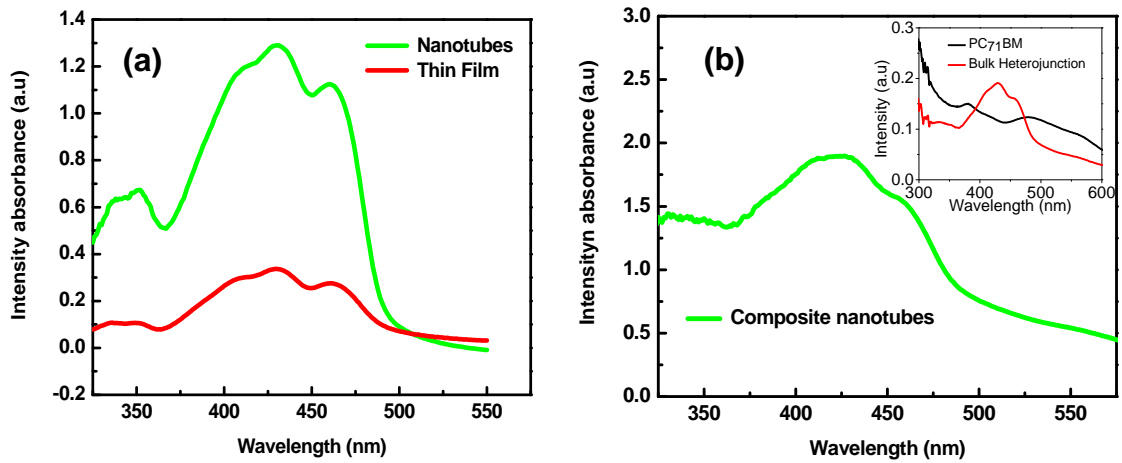


**Figure 6** UV-vis absorption spectra of (a) BHBT<sub>2</sub> thin films and nanotubes (b) BHBT<sub>2</sub> composite nanotubes and BHBT<sub>2</sub> bulk heterojunction, PC<sub>71</sub>BM thin films (inset).

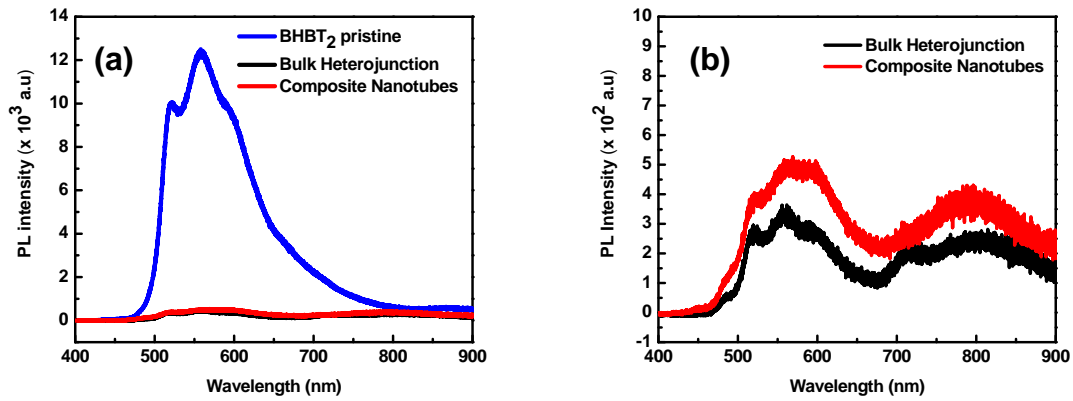


**Figure 7** (a) Photoluminescence spectra of BHBT<sub>2</sub> thin films, bulk heterojunction and composite nanotubes. (b) Photoluminescence comparison spectra between BHBT<sub>2</sub> bulk heterojunction and composite nanotubes.

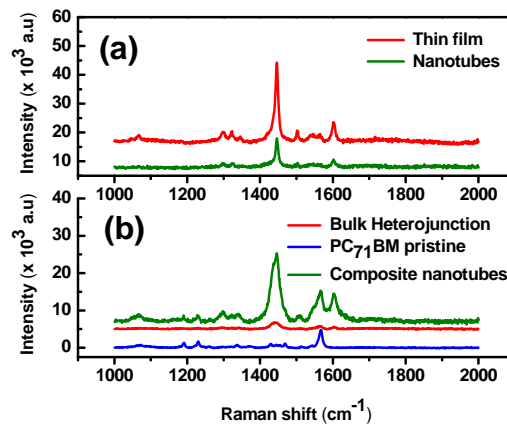


**Figure 8** (a) Raman spectra of BHBT<sub>2</sub> thin films and composite nanotubes. (b) Raman spectra of BHBT<sub>2</sub> bulk heterojunction, composite nanotubes and PC<sub>71</sub>BM.

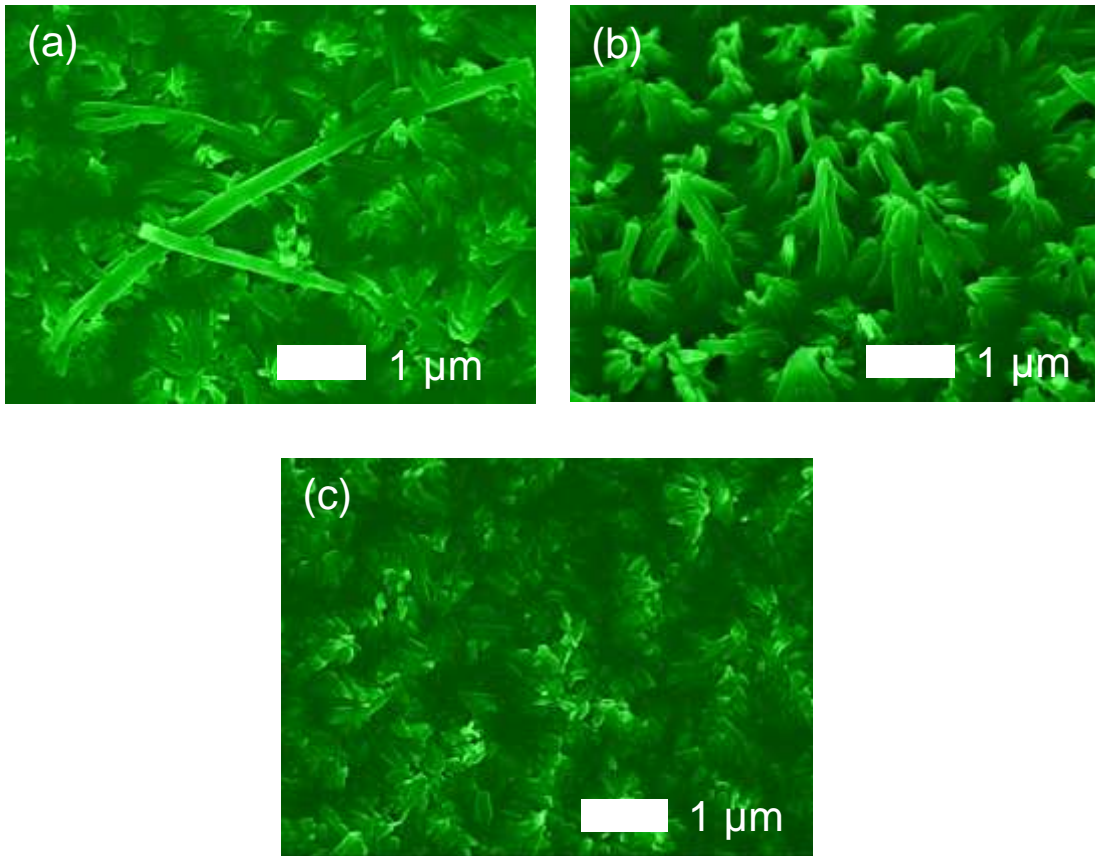


**Figure 9** FESEM images of BHBT<sub>2</sub> nanotubes at spin coating rate of (a) 1000 rpm (b) 2000 rpm (c) 3000 rpm.

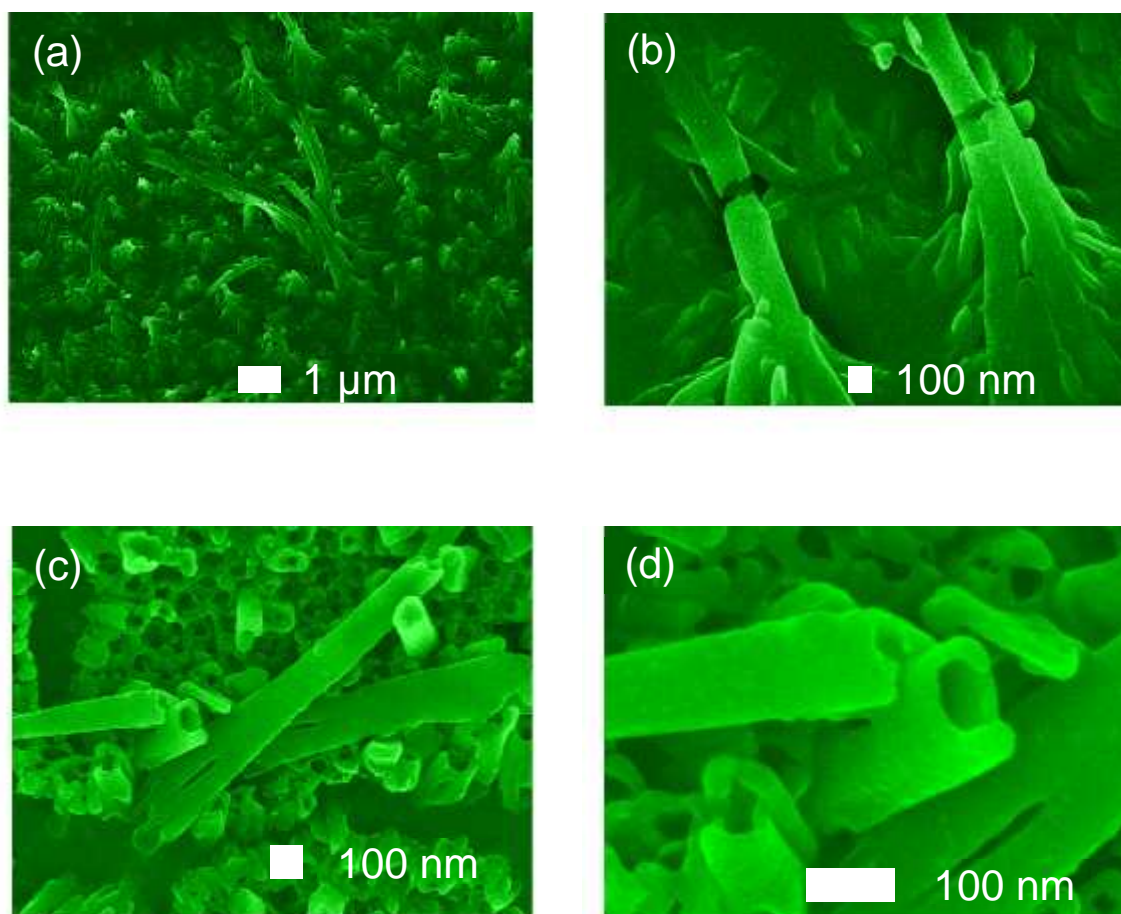


**Figure 10** (a) and (b) FESEM images of BHBT<sub>2</sub> nanotubes spin-coated at 2000 rpm. (c) and (d) FESEM images of BHBT<sub>2</sub>:PC<sub>71</sub>BM composite nanotubes spin-coated at 2000 rpm.

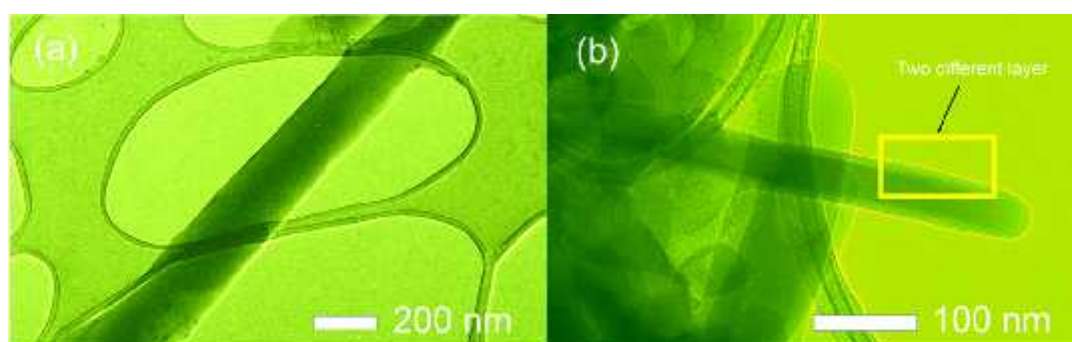


**Figure 11** HRTEM images of (a) BHBT<sub>2</sub> nanotubes (b) BHBT<sub>2</sub>:PC<sub>71</sub>BM composite nanotubes.



**Table 1** Raman peak positions of BHBT<sub>2</sub> and BHBT<sub>2</sub> : PC<sub>71</sub>BM [62]

Raman Shift				
BHBT <sub>2</sub>		BHBT <sub>2</sub> PC <sub>71</sub> BM		
Thin Film (at 2000 rpm)	Nanotubes (at 2000 rpm)	Bulk heterojunction (at 2000 rpm)	Composites Nanotubes (at 2000 rpm)	Vibrational Assignments
1067	1068	1067	1068	C=S stretch Ethylene trithiocarbonate
-	-	1188	1189	Ring "breathing"
-	-	1227	1231	Ring vibration Para-disubstituted benzenes
1297	1299	1295	1299	CC bridge bond stretch
1324	1325	1328	1322	Ring vibration
1344	-	1342	1338	CH deformation
1445	1446	1443	1443	Ring stretch 2- Substituted thiophenes
1503	1503	1507	1505	Symmetric C=C stretch
1544	1544	-	-	C=C stretch
1566	1564	1565	1567	C=C stretch
1601	1602	1603	1604	C=C stretch